Calculation of Transonic Rotor Noise Using a Frequency Domain Formulation

J. Prieur*
Office National d'Etudes et de Recherches Aérospatiales, Châtillon, France

This paper presents a formulation of the prediction of transonic quadrupole rotor noise in hover using a frequency domain method. The technique is applied to compute the high-speed noise of a model rotor. Tests on the computational stability of the method are presented and theoretical results are compared with published experimental data. Noise predictions on rotors with swept-tip blades are discussed.

I. Introduction

THE tendency to increase the forward speed of helicopters comes up against increases in main rotor noise. Flight tests have shown that the main rotor radiates intense impulsive noise at high forward speed, for which the advancing blade operates in transonic conditions. A close connection becomes necessary between aerodynamic and acoustic investigations in order to design new blade tips that meet the regulation requirements.

Until now, predictions on transonic blade noise have been based on Lighthill's aerodynamic sound theory and proceeded by integration of the Ffowcs, Williams, and Hawkings equation.

Linear calculations of the thickness and loading noise terms[1-3] were in poor agreement with experiment at high speed, leading researchers to take into account, in different ways, nonlinear effects.[1,4-7] The studies in Refs. 6 and 7 were based on acoustic analogy. In these references, the volume distribution of the quadrupole term of the Lighthill's stress tensor was evaluated using an aerodynamic code and included as an additional source in noise calculations. From transonic small disturbance (TSD) results, Schmitz and Yu[6] obtained a reasonable agreement between experiment and prediction for a hovering nonlifting rotor up to a tip Mach number of 0.9. Overprediction was observed at and above 0.9, leading research to focus on improving the near field data.[8]

Formulation[6] was written in the time domain. In a different way, far-field acoustic predictions using formulations in the frequency domain were done.[7,9-13] This approach avoids numerical differentiations and accordingly increases the accuracy of the results. Furthermore, as a consequence of far-field approximations, azimuthal integration can be performed analytically, which saves computation time. The present paper is an application of this kind of approach to evaluate, as a first step, the noise radiated by a thin, nonlifting, transonic rotor in hover.

High-speed impulsive noise mainly radiates in the forward direction, near the rotor plane. In this plane, it essentially is a combination of thickness and quadrupolar noises. The contribution of loading noise, which is weak because of its highly directive character (30 to 45 deg under the rotor plane) and the nonlifting hypothesis, is neglected. The quadrupolar noise is calculated in Sec. II. Sources are evaluated from chordwise and spanwise velocity disturbances calculated by means of a TSD potential code. Far-field and frequency domain formulas are used to integrate the elementary contributions. Nonlinear propagation is not considered.

An application to the rotor studied in Ref. 6 is presented in Sec. III. Calculated velocity disturbances are compared with the experimental results obtained by Yu et al.[14] Monopolar noise calculated at ONERA[11,12] and quadrupolar noise are added in order to compare with theoretical[6,15] and experimental[6] data.

Examples of noise predictions on rotors with swept-tip blades are presented in Sec. IV.

II. Calculation of the Quadrupolar Far-Field Radiation of a Hovering Rotor

Predicting transonic rotor noise in forward flight requires a lot of computation time and a large amount of computer memory. As a first step, this problem is approached with the study of the hovering case, in which blade tip transonic conditions are simulated by considering a rotational tip Mach number of the same order as that of the advancing blade of rotors in high-speed forward flight.

A. Basic Equations

It is known from Lighthill's analysis that density fluctuations ρ' that occur in a moving flow are the same as those that would result from a quadrupole source distribution of strength T_{ij} in a fictitious fixed acoustic medium of sound speed a_0 with

$$T_{ij}=\rho u_i u_j+(p-a_0^2\rho)\delta_{ij} \tag{1}$$

In the present case of a hovering rotor interacting with a fluid initially at rest, u_i and u_j are velocity disturbances.

The solution of Lighthill's equation, when interactions with solid surfaces (rotor blades) are involved, can be expressed[16] as

$$\rho'=\frac{1}{a_0^2}\int_{V(\tau)}\int_{\tau}\frac{\partial^2 G}{\partial y_i\partial y_j}T_{ij}\,\mathrm{d}\vec{y}\,\mathrm{d}\tau+\frac{1}{a_0^2}\int_{\tau}\int_{S(\tau)}\frac{\partial G}{\partial y_i}f_i\,\mathrm{d}S(\vec{y})\,\mathrm{d}\tau$$
$$+\frac{1}{a_0^2}\int\int_{S(\tau)}\rho_0 V_n\frac{\partial G}{\partial\tau}\,\mathrm{d}S(\vec{y})\,\mathrm{d}\tau \tag{2}$$

where V is a source integration volume supposed localized enough to allow integration and S is the surface of the blades. Equation (2) appears as a sum of three terms, respec-

Presented as Paper 86-1901 at the AIAA 10th Aeroacoustic Conference, Seattle, WA, July 9-11, 1986; received Sept. 8, 1986; revision received April 1, 1987.

*Research Engineer, Aeroacoustics Department.

tively known as quadrupolar noise (related to stresses), loading noise (associated with forces exerted by the blades on the fluid), and thickness or monopolar noise (related to the fluid mass fluctuations due to the blades). We will not deal with the second term.

B. Evaluation of Source Terms

The knowledge of the Lighthill's stress tensor requires the calculation of the components of the fluid velocity. This is done by means of the ONERA nonviscous TSD code (developed by ONERA and the U.S. Army Aeromechanics Laboratory[17] within the framework of a memorandum of understanding on helicopters and later extended).[18]

The exact value of ρ and the second $(p-a_0^2\rho)\delta_{ij}$ term in T_{ij} are expressed from the fluid disturbance velocity by means of classical TSD calculations.

Finally,

$$\rho \simeq \rho_0(1-u_1\cdot M_T\cdot \eta_2/R)$$

$$(p-a_0^2\rho) \simeq [(\gamma-1)/2]\rho_0 u_1^2 (M_T\cdot \eta_2/R)$$

C. Far-Field Formulation

A classical far-field expression for the acoustic quadrupolar pressure at a fixed (referred to rotor-axis) observer's position can be derived from the first integral of Eq. (2)

$$p'(\vec{x}, t) = \frac{1}{a_0^2}\frac{\partial^2}{\partial t^2}\int_V \int_\tau T_{RR}(\vec{x}, \vec{y}, \tau) \times G(\vec{x}, t\,|\,\vec{y}, \tau)\,d\vec{y}\,d\tau \tag{3a}$$

where $T_{RR} = T_{ij}(r_i r_j/r^2)$, see the geometry in Fig. 1.

Taking the Fourier transform of p' vs t, we obtain the Fourier component of the acoustical pressure

$$P'(f, \vec{x}) = -\frac{(2\Pi f)^2}{a_0^2}\cdot\frac{B}{T}\int_V \int_\tau \frac{T_{RR}}{4\Pi r} \times e^{-i2\Pi f(\tau + r/a_0)}d\vec{y}\,d\tau \tag{3b}$$

Changing τ into ψ/Ω and using blade-attached coordinates gives

$$P'(f_{mB}, \vec{x}) = -B\frac{k_{mB}^2}{2\Pi}\int_V \int_{\psi=0}^{2\Pi} \frac{T_{RR}(\vec{x}, \vec{\eta}, \psi)}{4\Pi r} \times e^{-i(k_{mB}r + mB\psi)}d\psi\,d\vec{\eta} \tag{4}$$

When Eqs. (3b) and (4) are compared with corresponding expressions in Refs. 4 and 6, two simplifications brought by the frequency domain formulation appear.

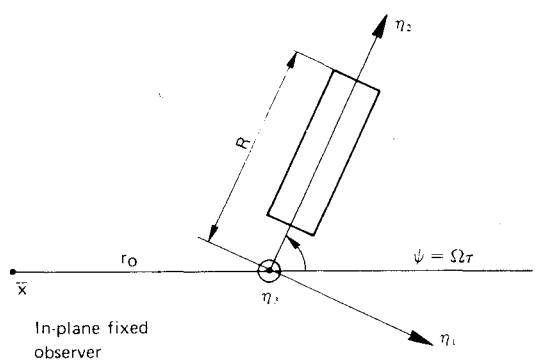

Fig. 1 Geometry.

First, no singularity is explicitly present in the integrand of Eq. (3b), unlike time domain formulas[4,6] that exhibit a singular Doppler factor $(1/1-M_R)$. This was underscored in the past.[1]

Second, time domain formulations require the evaluation of retarded emission times for each source location in the moving frame by solving an implicit equation with the multiple roots depending on M_R values. Here, the integration vs τ of Eq. (3b) is performed over an entire revolution of the source. Furthermore, the corresponding (0, 2Π) integration of ψ in Eq. (4) can be carried out analytically by means of Bessel functions, which saves computation time.

Calculation can be simplified if the far-field observer is assumed to be located in the rotation plane where high-speed sound radiation is maximum. Then, in-phase integration of the source intensities in the η_3 direction is possible, reducing the quadrupole volume integration to a surface integration in the rotor plane.

By neglecting the contribution of velocity disturbance u_3 normal to the blade planform, we define

$$T_{11} = \int \rho u_1^2 d\eta_3, \quad T_{12} = \int \rho u_1\cdot u_2 d\eta_3, \quad T_{22} = \int \rho u_2^2 d\eta_3$$

$$T_{00} = \int (p-a_0^2\rho)d\eta_3 = \int \left(\frac{\gamma-1}{2}\right)\cdot\rho_0 u_1^2\left(\frac{M_T\eta_2}{R}\right)^2 d\eta_3$$

By retaining only the terms of order $(|\eta|/r_0)$ in the phase factor, by neglecting them in the amplitude term and performing an analytical integration vs ψ, we get the final for-

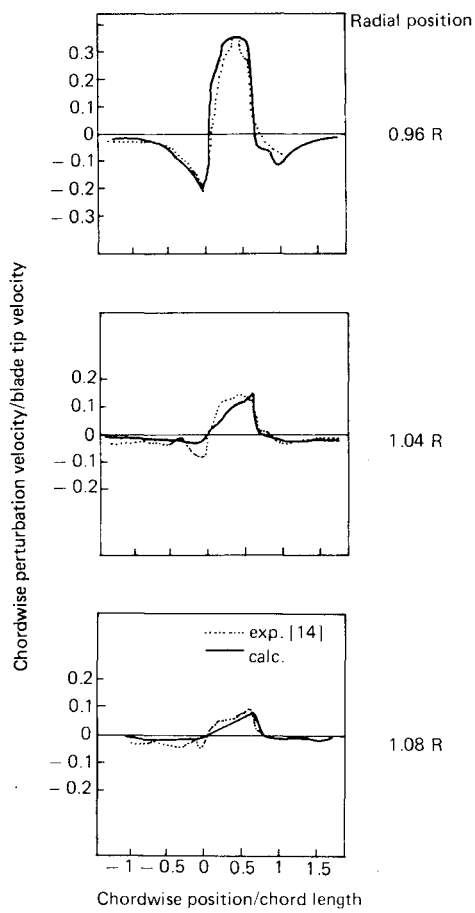

Fig. 2 Comparison between ONERA TSD-predicted velocity distributions and experimental Yu et al. results[14] (vertical distance to the rotor plane = 0.08 chord length).

mula, which is the main theoretical result of the paper:

$$P'(f_{mB}, \vec{x}) = -\frac{B \cdot k_{mB}^2}{8\Pi r_0} \cdot e^{-ik_{mB}(r_0 + mB(\Pi/2))} \times \int_{\eta_2} \int_{\eta_1} e^{-imB\eta_1/\eta_2} \left\{ (T_{11} + T_{22} + 2T_{00}) J_{mB}(k_{mB}\sqrt{\eta_1^2 + \eta_2^2}) + \left(\frac{T_{11} + 2iT_{12} - T_{22}}{2} \right) e^{2i\eta_1/\eta_2} \times J_{mB-2}(k_{mB}\sqrt{\eta_1^2 + \eta_2^2}) + \left(\frac{T_{11} - 2iT_{12} - T_{22}}{2} \right) \times e^{-2i\eta_1/\eta_2} \cdot J_{mB+2}(k_{mB}\sqrt{\eta_1^2 + \eta_2^2}) \right\} d\eta_1 \, d\eta_2 \quad (5)$$

The integration vs η_1 and η_2 is performed numerically (simplifications in the calculation of Bessel functions are done), and the time signatures are obtained by means of an inverse Fourier transform.

Interesting qualitative considerations may be deduced from Eq. (5). Let us set $n = mB$ and $k_n = n \cdot M_T/R$. The study of the behavior of the elementary Fourier component $\Delta P'(f_n, \Delta\eta, x)$ for large values of n allows us to distinguish two regions in the rotor plane, separated by the sonic circle $M_T|\eta|/R = 1$:

1) The inner region in which $M_T|\eta|/R < 1$, where $J_n(nM_T|\eta|/R)$ is of the order of $n^{-1/2} \cdot [f(M_T|\eta|/R)]^n$ with $f < 1$. The acoustic contribution of this region to the Fourier components of the acoustic pressure decreases exponentially as a function of n.

2) The outer region in which $M_T|\eta|/R \geq 1$, where $J_n(nM_T|\eta|/R)$ is of the order of $n^{-1/2} \cdot \cos[nM_T|\eta| \div R - (n + 1/2)\Pi/2]$. Then, $\Delta P'$ is an oscillating function of n, weighted by an increasing $n^{3/2}$ factor. Consequently, the convergence of integral (5) will strongly depend on phase compensations between the elementary radiations when the source integration area will extend to the region out of the sonic circle. To ensure this convergence, a sufficiently small chordwise mesh size of the acoustic code grid (of the order of a quarter of the minimum wavelength) must be chosen.

Furthermore, the noise contribution of the region near the sonic circle is potentially rich in high harmonics (which sharpen the signal) and can be dominant even if quadrupole intensities are rather weak. One can expect the occurrence of a radiating discontinuity (as it was recognized by Tam[19] for linear solutions of the high-speed rotor thickness noise problem), depending on the particular features of the flowfield related to a given blade tip. Accordingly, a precise evaluation of the sources in this region is needed, and tests on the influence of the extent of the source integration area have to be done.

III. Application to the UH-1H Model Rotor in Hover

The UH-1H model rotor has been studied extensively by the U.S. Army. Our noise evaluations are done in hover for the untwisted blades in order to compare them with previously published theoretical and experimental data.[2,6,14,15]

The characteristics of this rotor are the following: two blades; untwisted with rectangular planform; profile, NACA-0012 constant; radius $R = 1.045$ m; and, aspect ratio, 13.71.

Results corresponding to values of the rotational tip Mach number of 0.88, 0.90, and 0.92 are presented in detail. The case $M_T = 0.90$ is considered first. Theoretical results for the perturbation velocity distributions and for the acoustic signatures are presented.

A. Evaluation of the Perturbation Velocity Distribution at $M_T = 0.90$

The ONERA TSD code was run with a mesh of approximately 62,000 nodes: 85 in the chordwise η_1 direction (on $-8c$, $+6c$), 46 in the spanwise η_2 direction (on 0.5 to 1.5 R), and 16 in the η_3 direction (on $-6c$ to 0).

This number of nodes was found to be a compromise between moderate computation times and the requirements for a good accuracy of acoustic results. As explained at the end of Sec. II.C, the acoustic code needs a much smaller mesh size in the sensitive region: The intensities of sources at the nodes of the acoustic grid are evaluated by interpolation of the aerodynamic results.

A comparison between predicted and experimental TSD chordwise velocity perturbations obtained from holographic interferogram data by Yu et al.[14] at several radial locations is presented on Fig. 2. Correct agreement between theory and experiment is observed.

B. Quadrupolar Noise Predictions at $M_T = 0.90$

All results presented refer to an isolated blade; the corresponding signature for the two-bladed rotor is identical to that of the isolated blade except that it repeats with a periodicity of $T/2$ instead of T.

The acoustic pressure spectrum of the two-bladed rotor can be deduced from the spectrum of the isolated blade, corresponding to the even harmonics of the rotation frequency, by adding 6 dB, the overall sound pressure level (OASPL) being increased by 3 dB. In order to obtain a precise definition of signatures, the spectrum is calculated up to the 1024th harmonic of the rotation frequency (which cor-

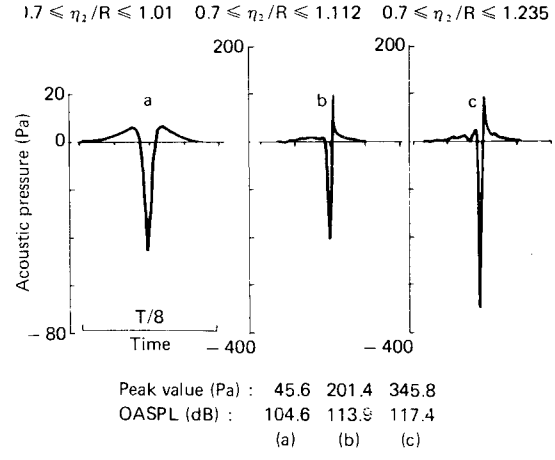

Fig. 3 Quadrupolar signatures as a function of the spanwise source extent, in-plane, $r_0 = 10R$, $M_T = 0.9$ $(-1.7 \leq \eta_1/c \leq 3.0)$.

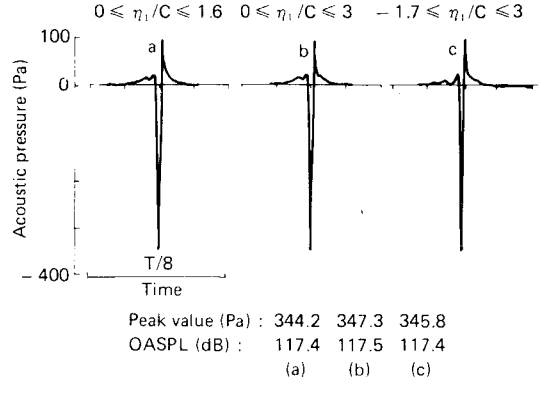

Fig. 4 Quadrupolar signatures as a function of the chordwise source extent, in-plane, $r_0 = 10R$, $M_T = 0.9$ $(-0.7 \leq \eta_2/R \leq 1.23)$.

responds for the real rotor to a maximum frequency of 7 KHz).

With the requirement that the mesh size of the acoustic grid be of the order of magnitude of a quarter of the minimum wavelength, the following extent of the source area is considered: $-1.7 \leq \eta_1/c \leq 3.0$ and $0.7 \leq \eta_2/R \leq 1.23$.

1. Study of the Influence of the Extent of the Source Integration Area in the Rotation Plane

Influence of the spanwise extent. Calculations are done at a distance of $10R$ from the rotor-hub in order to match with our far-field approximation's requirement.

The evolution of the signatures, as the source spanwise integration extent increases (the chordwise one remaining unchanged), is presented in Fig. 3. As shown in Fig. 3a, the contribution of the region $\eta_2 < R$ is symmetrical in time and of weak amplitude, whereas that of the region near the sonic circle is very saw-tooth in character (see Fig. 3b), which suggests that the high-order harmonics content is more important in Fig. 3b than in Fig. 3a. This illustrates the remarks made at the end of Sec. II.

It has been found that extending the source integration up to $\eta_2 = 1.23R$ was sufficient to obtain a computationally stable result (as an example, integration up to $1.28R$ resulted in a prediction differing from prediction 3c only by +0.1 dB).

Influence of the chordwise extent. Figure 4 shows the acoustic results corresponding to increasing chordwise extents of the source area.

From Figs. 4a and 4c, the contribution of the additional sources of weak intensities involved in successive calculations appears quite low. The main result is that a satisfactory computational stability is observed (even after addition of monopolar noise) as the source chordwise extent is increased, contrary to the results of Ref. 15.

2. Contribution of Different Source Terms

We have found that neglecting the contributions from the $\rho u_1 u_2$ and ρu_2^2 terms of the Lighthill's stress tensor decreases the amplitude of the negative pressure peak by 15%. Consequently, these terms are taken into account in our predictions (unlike Refs. 6 and 15).

C. Addition of the Monopolar Contribution and Comparison to Previous Results

In order to evaluate the total high-speed noise in the rotation plane, we add to each complex quadrupolar Fourier component the in-phase monopolar one calculated by Caplot[11,12] and carry out an inverse Fourier transform to get the resulting time signatures. Our results are extrapolated to a distance $r_0 = 3R$, with us assuming a $1/r_0$ decay of the acoustic pressure, in order to compare with published experimental data.

1. $M_T = 0.88$

The total noise is shown in Fig. 5 and compared in Fig. 6 with experimental results.[6]

Figure 5 shows that monopolar and quadrupolar contributions are of the same order of magnitude but different in shape: The first is symmetrical in time, whereas the second is asymmetrical and sharper. Correspondingly, the quadrupolar spectrum contains more high harmonics but still has a rapidly decreasing level.

2. $M_T = 0.90$

Figure 7 shows that the quadrupolar contribution is much increased compared with the monopolar one (the amount of which is only 20% in amplitude of the total pulse), whereas its asymmetrical character is reinforced. As was pointed out by Schmitz and Yu, it is a consequence of the fact that shocks, which have an exclusively local character until

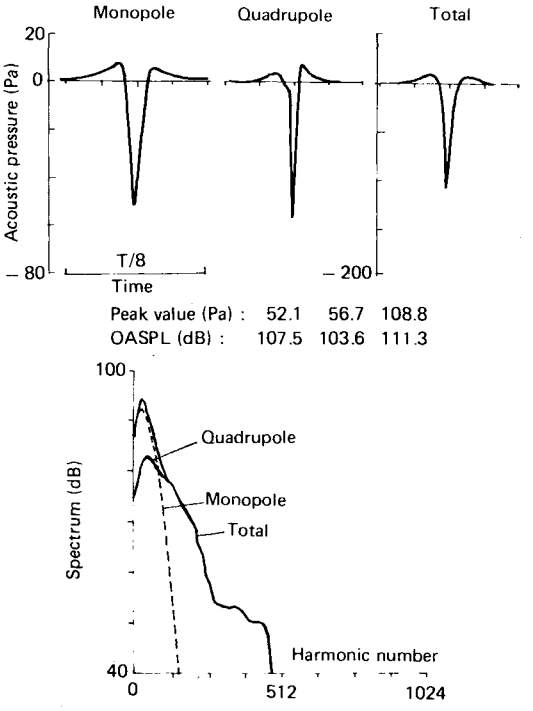

Fig. 5 Acoustic prediction, in-plane, $r_0 = 10R$, rectangular blade, $M_T = 0.88$.

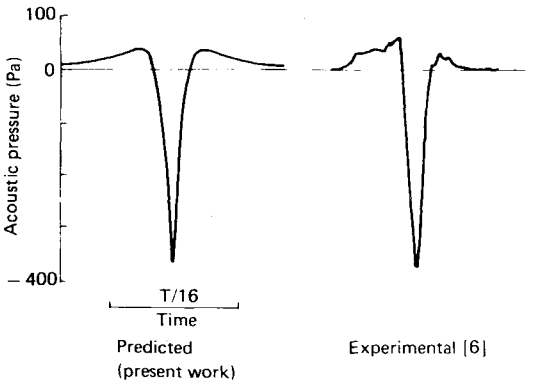

Fig. 6 Acoustic theory-experiment comparison, $r_0 = 3R$, rectangular blade, $M_T = 0.88$.

$M_T = 0.88$, suddenly begin to propagate to the acoustic far field, a phenomenon called "delocalization." This point will be illustrated in Sec. IV.

Figure 8 shows a comparison between our prediction, theoretical ones,[6,15] and experimental results at $r_0 = 3R$. In every case, the theory overpredicts the amplitude of the negative pressure peak: Our calculation, as Aggarwal's,[15] overpredicts it by a factor of 2. But unlike those of Ref. 15, our results are not dependent on the extent of the integration area of sources.

Our positive peak value is rather low; this could be a consequence of the inaccuracy of quadrupole computed values near the sonic circle.

3. $M_T = 0.92$

Predictions are presented in Fig. 9. Compared with Figs. 5 and 7, the contribution of monopolar noise is found to become nearly negligible in regard to total in-plane OASPL. The main reason is that the monopolar spectrum extends only up to approximately 200 harmonics. On the contrary, the quadrupolar one decreases only very slightly as frequency increases: The levels of the highest harmonics are certainly

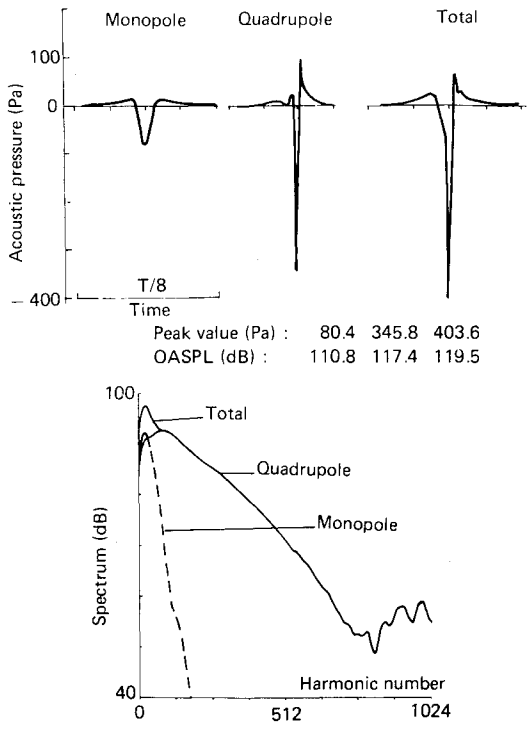

Fig. 7 Acoustic prediction, in-plane, $r_0 = 10R$, rectangular blade, $M_T = 0.9$.

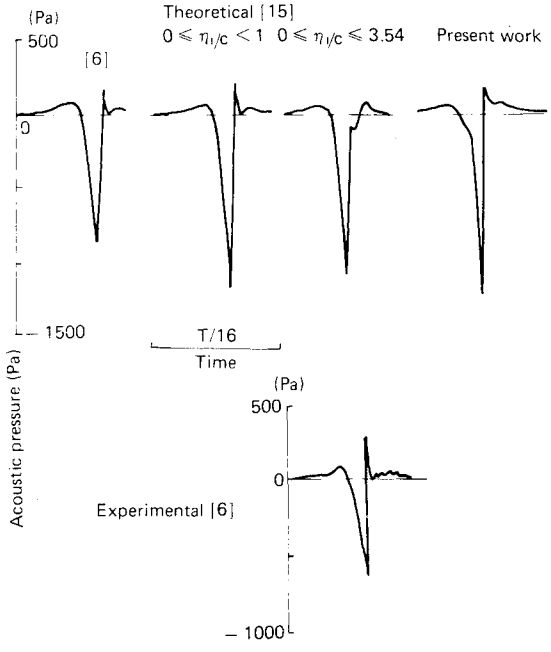

Fig. 8 Acoustic theory-experiment, comparison, in-plane, $r_0 = 3R$, rectangular blade, $M_T = 0.9$.

overpredicted as a consequence of the too wide size of the calculation grid with respect to the wavelength.

A final comparison between theory and experiment is presented in Fig. 10. It shows a good agreement for Mach numbers up to 0.9, but overprediction at and above 0.9, exactly as in Ref. 6. This point will be discussed in Sec. V.

IV. Application to Nonrectangular Blades: Hovering Case, $M_T = 0.9$

This method is applied to a fictitious rotor fitted with two different nonrectangular tips and of the same aspect ratio and radius as the UH-1H model rotor.

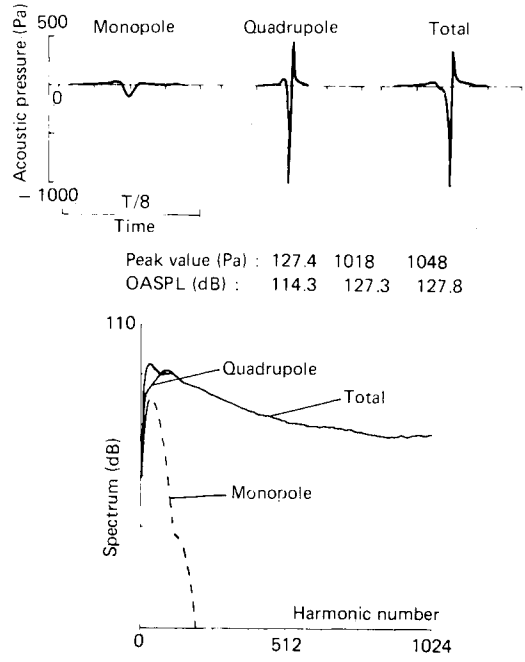

Fig. 9 Acoustic prediction, in-plane, $r_0 = 10R$, rectangular blade, $M_T = 0.92$.

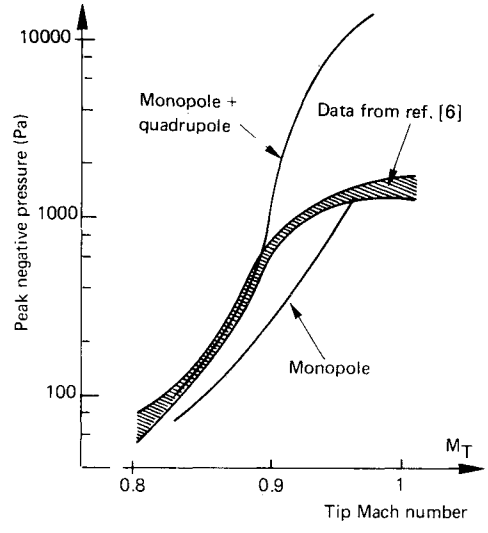

Fig. 10 Theory-experiment comparison, in-plane, $r_0 = 3R$, rectangular blade.

The chord profile of the blades is still a NACA-0012. The different tips are represented on Fig. 11; they are a swept-back tip of 30 deg, between $0.95R$ and R (F30) and a progressive swept tip with taper (PF2) (a precise definition of this ONERA designed tip can be found in Ref. 20).

The iso-Mach lines obtained from TSD calculations, together with predicted signatures, are presented respectively in Figs. 12, 13, and 14 for the rectangular F30 and PF2 blades.

Corresponding predicted OASPL for isolated blades at 10 R are 119.5, 118.8, and 110.5 dB. The 0.7 dB reduction of noise obtained with F30 is due to a reduction in monopolar noise, the qudrupolar contribution being of the same order as that of the rectangular blade. An important gain is obtained with the PF2 tip, because of a nearly negligible quadrupolar noise.

Figure 14 shows that delocalization phenomena have not yet occurred on PF2 at $M_T = 0.9$ unlike the other tips. Referring to the sonic cylinder $M = 1$, the inner supersonic region

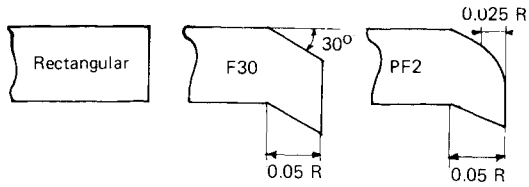

Fig. 11 Different tip shapes.

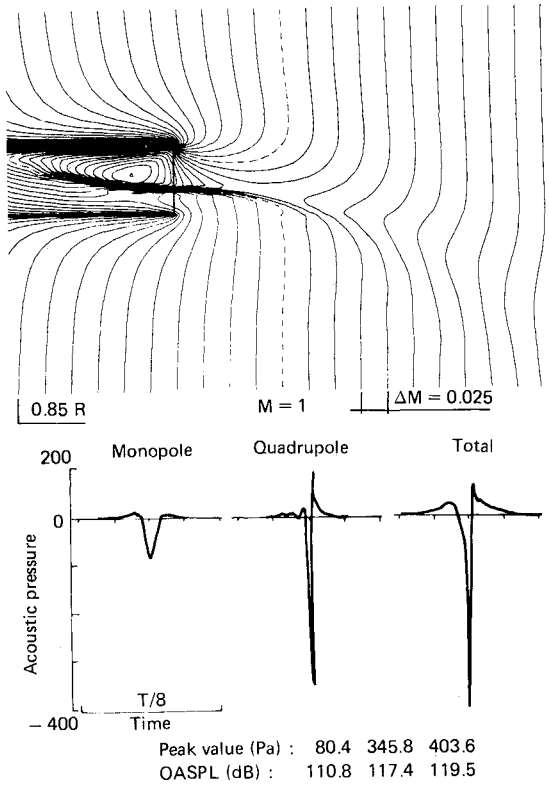

Fig. 12 Iso-Mach lines and predicted signatures, in-plane, $r_0 = 10R$, rectangular tip, $M_T = 0.9$.

(on the blade) is disconnected with the outer one. Between these, there is a wide area in which the potential equation is elliptic with no wavelike behavior: no propagation is allowed for a perturbation coming from the inner hyperbolic region toward the sonic surface. The nearly negligible quadrupolar signature of the PF2 tip illustrates this fact.

V. Discussion

As shown in Sec. II, the acoustic prediction is strongly dependent on the accuracy of the near-field input data, particularly near and beyond the sonic circle. The TSD code, originally designed for aerodynamic purposes, is well adapted to obtain results on the blade extent but not away from the blade tip. Indeed, as shown in Ref. 8, the TSD code based on finite-difference shock-capturing methods results in smearing the shocks over several grid points, this effect being more and more pronounced as the distance from the blade tip is increased: This may partly explain the discrepancy between theory and experiment at and above $M_T = 0.9$.

Furthermore, this numerical effect may have affected the tests we did in Sec. III.B.1 on the spanwise extent of the source volume to be taken into account. Similar tests and noise predictions at different tip Mach numbers from the results of a more sensitive aerodynamic code would have therefore to be performed to assess the influence of the accuracy of input source data on noise prediction and to evaluate the possibilities of the method.

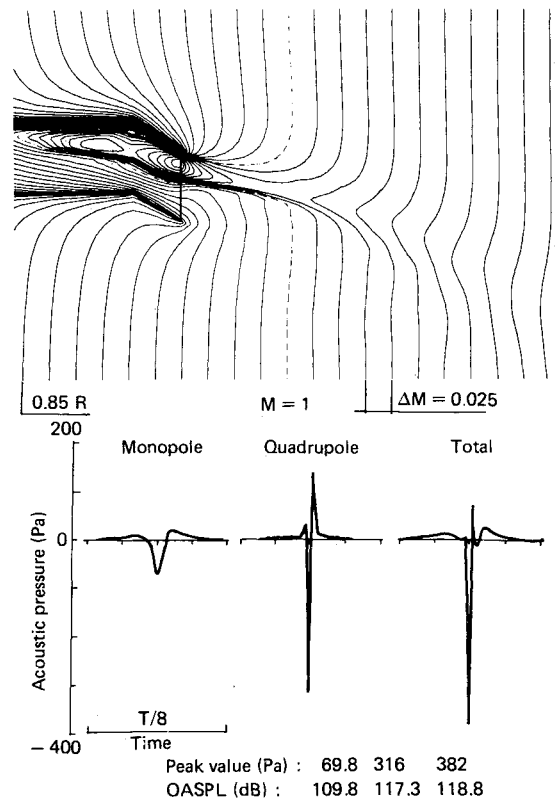

Fig. 13 Iso-Mach lines and predicted signatures, in-plane, $r_0 = 10R$, F30 tip, $M_T = 0.9$.

Besides the requirement for sufficiently accurate input near-field data, the fundamental question of the validity of the method arises. Several authors[4,21] have criticized calculations of transonic rotating blade noise based on Lighthill's acoustic analogy by taking into account quadrupole sources. The overprediction of noise above the delocalization point, shown in Fig. 10, causes us to call into question calculations of this kind in the conditions of delocalization.

To be of practical interest, predictions based on acoustic analogy have to assume the quadrupole integration volume to be localized (see Sec. II). This hypothesis allows us to use far-field approximations, provided that the observer is located far from the sources.

In fact, once a shock radiates, the hypothesis of a source volume localized enough to not include the observer's location becomes questionable. It is of interest to investigate the consequences of such a hypothesis by examining Eq. (5).

In this equation, a Fourier component of the acoustic pressure is expressed, due to far-field approximations, as a product of an integral over the source extent (independent of the observer's location) by a $e^{-ik_{mB}r_0}/r_0$ factor.

A consequence of the aforementioned hypothesis is thus that the acoustic wave reduces to a spherical wave propagating at a constant speed without any distortion, contrary to what is known of nonlinear noise propagation in transonic conditions.

Finally, the far-field approximation is invalidated by nonlinear shock-propagation effects that become more and more important as the tip Mach number is increased above the delocalization tip Mach number. Calculations of transonic rotor noise based on the present approach thus appear to be of limited validity.

In the presence of sufficiently intense shocks, a practical way seems to be in a combination of near-field calculations coupled with a nonlinear propagation model.

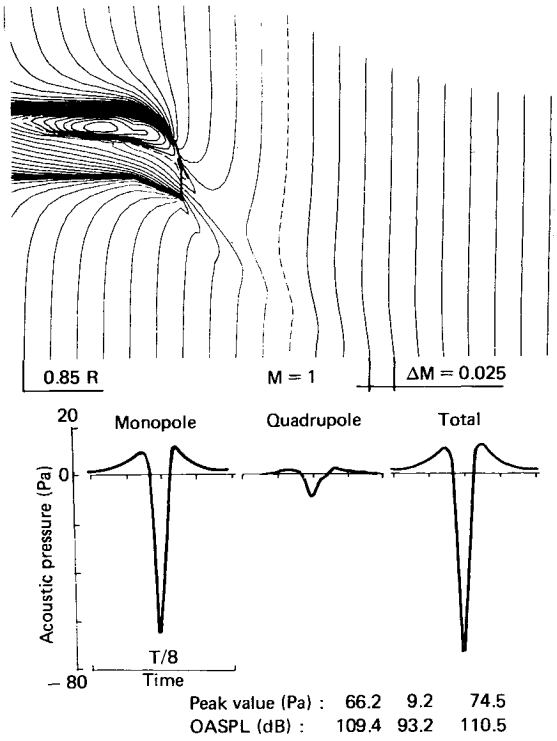

Fig. 14 Iso-Mach lines and predicted signatures, in-plane, $r_0 = 10R$, PF2 tip, $M_T = 0.9$.

VI. Conclusions

Predictions of transonic rotor noise based on the quadrupole approach and using a frequency domain formulation agree with similar calculations in the time domain. The Fourier transform technique simplifies the calculations. On the other hand, to obtain sufficient accuracy, complex Fourier components must be evaluated up to a large number of harmonics of the rotation frequency.

Good agreement is obtained between experiment and our theory on the rectangular blades at hovering tip Mach numbers lower than the delocalization tip Mach number, but overprediction is observed at and above this point, as in time domain calculations.

The discrepancy between prediction and experiment may be partly explained by inaccurate near-field input data: This will be investigated by running the acoustic code with source values obtained from an improved aerodynamic code. Nevertheless, a more fundamental cause of overprediction is that this quadruple approach of transonic rotor noise is inadequate in the presence of sufficiently intense shock waves.

As a consequence, another method has to be found to assess rotor noise in the presence of shock waves. Implementation of this method will need to progress in near-field aerodynamic calculations.

Acknowledgments

This work is supported by a grant from Service Technique des Programmes Aéronautiques, and we thank O. Lambert for his interest in the present study. We are grateful to the ONERA Aerodynamics Department for its help in computations, mainly to J. J. Philippe and A. Desopper for their assistance in running the TSD code and their fruitful suggestions.

References

[1]Hawkings, D. L. and Lowson, M. V., "Theory of Open Supersonic Rotor Noise," *Journal of Sound and Vibration*, Vol. 36, No. 1, 1974, pp. 1–20.

[2]Boxwell, D. A., Yu, Y. H., and Schmitz, F. H., "Hovering Implusive Noise: Some Measured and Calculated Results," *Vertica*, Vol. 3, No. 1, 1979, pp. 33–45.

[3]Farassat, F., Nystrom, P. A., and Morris, C. E. K. Jr., "A Comparison of Linear Acoustic Theory with Experimental Noise Data for a Small Scale Hovering Rotor," AIAA Paper 79-0608, Seattle, WA, 1979.

[4]Isom, M. P., "Some Non-Linear Problems in Transonic Helicopter Acoustics," Poly M/AE Rept. 79-19, Polytechnic Institute of New York, May 1979.

[5]Hawkings, D. L., "Noise Generation by Transonic Open Rotors," Westland Helicopters Limited, Yeovil, Somerset, Research Paper 599, July 1979.

[6]Schmitz, F. H. and Yu, Y. H., "Transonic Rotor Noise—Theoretical and Experimental Comparisons," 6th European Rotorcraft and Powered Lift Aircraft Forum, Paper 22, Bristol, England, Sept. 1980.

[7]Hanson, D. B. and Fink, M. R., "The Importance of Quadrupole Sources in Prediction of Transonic Tip Speed Propeller Noise," *Journal of Sound and Vibration*, Vol. 62, No. 1, 1979, pp. 19–38.

[8]Rutherford, J. W., "Shock Fitting Applied to the Prediction of High-Speed Rotor Noise," 11th European Rotorcraft and Powered Lift Aircraft Forum, Paper 8, London, England, Sept. 1985.

[9]Dahan, C., Avezard, L., Guillien, G., Malarmey, C., and Chombart, J., "Propeller Light Aircraft Noise at Discrete Frequencies," *Journal of Aircraft*, Vol. 18, June 1981, pp. 480–486.

[10]Dahan, C. and Gratieux, E., "Helicopter Rotor Thickness Noise," *Journal of Aircraft*, Vol. 18, June 1981, pp. 487–494.

[11]Caplot, M., "Calcul du bruit de raies émis par un rotor d'hélicoptere en champ lointain," Ph.D. Thesis, Université de Compiegne, Dec. 1985.

[12]Lévy, S. and Caplot, M., "Helicopter Noise," Lecture Series of the Von Karman Institute on Aeroacoustics: Ten Years of Research, Rhode St. Genese, April 1983.

[13]Hanson, D. B., "Near-Field Frequency-Domain Theory for Propeller Noise," AIAA Paper 83-0688, April 1983.

[14]Yu, Y. H., Kittleson, J. K., and Becker, F., "Reconstruction of a Three-Dimensional Transonic Rotor Flow Field from Holographic Interferogram Data," 41st AHS Annual Forum, Fort Worth, TX, May 1985.

[15]Aggarwal, H. R., "The Calculation of Transonic Rotor Noise," *AIAA Journal*, Vol. 22, July 1984, pp. 996–998.

[16]Goldstein, M. E., *Aeroacoustics*, Mc-Graw-Hill, New York, 1976.

[17]Chattot, J. J., "Calculation of Three-Dimensional Unsteady Transonic Flows Past Helicopter Blades," NASA TP 1721 and AVRADCOM TR 80-A-2, Oct. 1980.

[18]Desopper, A., Lafon, P., Ceroni, C., and Philippe, J. J., "Ten Years of Rotor Flow Studies at ONERA," 42nd AHS Annual Forum, Washington, DC, June 1986.

[19]Tam, C. K. W., "On Linear Acoustic Solutions of High-Speed Helicopter Impulsive Noise Problems," *Journal of Sound and Vibration*, Vol. 89, No. 1, 1983, pp. 119–134.

[20]Guillet, J. and Philippe, J. J., "Flight Test of a Sweptback Parabolic Tip on a Dauphin 365 N," 10th European Rotorcraft Forum, The Hague, the Netherlands, 1984.

[21]Morris, C. E. K. Jr., Farassat, F., and Nystrom, P. A., "An Evaluation of Linear Acoustic Theory for a Hovering Rotor," NASA TM 80059, May 1979.